Concise Report

N-Oxides, Osmium, Pincer, Carbolong, Metallacycles, Density functional calculations

CJC Chinese Journal of Chemistry 中国化学 An International Journal

The First OCCCO Pentadentate Chelates: Osmium Mediated Stepwise Oxidations of Terminal Alkynes by Pyridine *N*-Oxide

Jianfeng Lin,[a,b] Qiannan Xu,[a] Xinlei Lin,[a] Yuhui Hua,[a] Dafa Chen,[b] Yonghong Ruan,[a] Hong Zhang,*[,a] and Haiping Xia*[,a,b]

[a] *College of Chemistry and Chemical Engineering, Xiamen University, Xiamen, Fujian 361005, China*
[b] *Shenzhen Grubbs Institute, Department of Chemistry, Guangdong Provincial Key Laboratory of Catalysis, Southern University of Science and Technology, Shenzhen, Guangdong 518055, China*

Cite this paper: *Chin. J. Chem.* **2020**, *38*, 1273—1279. **DOI: 10.1002/cjoc.202000227**

Summary of main observation and conclusion Oxygen atom transfer reactions between alkynes and heteroarene *N*-oxides are currently mediated by transition metal, such as gold, ruthenium or rhodium, but they have never been catalyzed by osmium. Herein, we report stepwise oxidations of terminal alkynes mediated by an osmium carbolong complex, using pyridine *N*-oxide as the oxidant, yielding novel aldehyde- or carboxylic acid-coordinated osmapentalyne derivatives selectively. The mechanism was illustrated by density functional theory calculations, providing a new route for oxygen atom transfer between heteroarene *N*-oxides and alkynes.

Background and Originality Content

Heteroarene *N*-oxides are powerful reagents for the transition metal mediated oxygen atom transfer reactions of alkynes in the synthesis of carbonyl compounds.[1] In the case of terminal alkynes, generally, there are two reaction patterns (Scheme 1). As shown in path a, for gold-catalyzed reactions, they usually initially lead to α-oxo gold carbenes followed by nucleophilic attack to afford β-carbonyl compounds.[2] In the other pattern, terminal alkynes firstly react with metal (mostly Rh or Ru catalyst) to yield vinylidenes. After the oxidation by heteroarene *N*-oxides, metallaketene intermediates are produced, which are further attacked by nucleophiles or unsaturates to give α-carbonyl compounds and cyclic carbonyl compounds, respectively.[3] On the other hand, the conversion of terminal alkynes to aldehydes oxidized by heteroarene *N*-oxides has been rarely reported. In 2011, Gagosz *et al*. discovered a Cu(I) catalyzed transformation from alkynyl oxiranes and oxetanes to functionalized five- or six-membered α,β-unsaturated lactones or dihydrofuranaldehydes in the presence of pyridine *N*-oxide, in which an intramolecular annulation occurs *via* a nucleophilic attack (Scheme 2).[4] The other example was reported by Liu and coworkers in 2013.[5] They found a distinct chemoselectivity in the gold-catalyzed oxidative cyclization of 3,5-dien-1-ynes when using 3,5-dichloropyridine *N*-oxide as the oxidant, generating cyclopentadienyl aldehydes as products. In this case, the annulation takes place through the attack of the alkenyl group that links with R^3 and R^4 (Scheme 2).

The above-mentioned oxygen atom transfer reactions are still limited in organic systems. If such transformation could be expanded to organometallics, not only unprecedented structures, but also crucial intermediates, might be isolated. As a part of our ongoing research interest in carbolong chemistry,[6] we considered complex **1** as a suitable candidate, not only because its highly reactive Os-C(sp^3) group might play an analogous role as the oxygen atom in Gagosz's system and the alkenyl group in Liu's reactions, but also due to its diversiform reactivities with alkynes.[7] Thus, the reactions of **1** with terminal alkynes in the presence of pyridine *N*-oxide were tested, and several interesting osmapentalynes with an coordinated aldehyde group were achieved through an intermolecular annulation process, confirming our assumption (Scheme 2). Importantly, no additional catalyst is required in contrast to the traditional organic reactions. Furthermore, density functional theory (DFT) calculations were described to illustrate the reaction mechanism, disclosing a new route in heteroarene *N*-oxide initiated oxygen atom transfer reactions. Notably, the coordinated aldehydes could be further converted to carboxylic complexes conveniently with the addition of excess

Scheme 1 Heteroarene *N*-oxides initiated oxygen atom transfer reactions of terminal alkynes mediated by transition metals

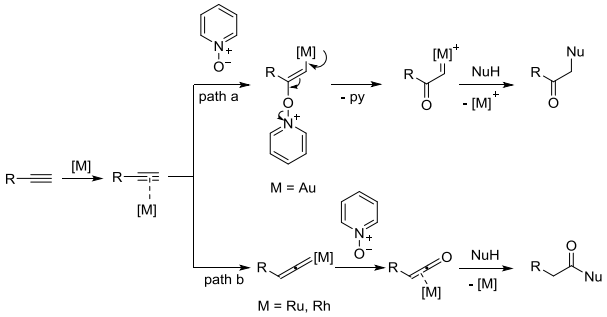

Scheme 2 Conversion of terminal alkynes to aldehydes oxidized by heteroarene *N*-oxides

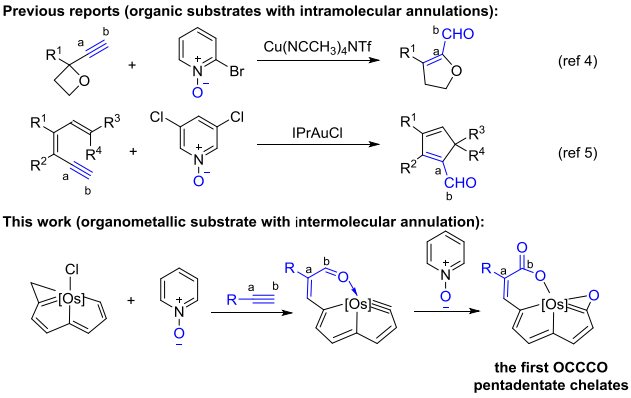

*E-mail: zh@xmu.edu.cn, hpxia@xmu.edu.cn

For submission: https://mc.manuscriptcentral.com/cjoc
For articles: https://onlinelibrary.wiley.com/journal/16147065

pyridine *N*-oxide, accompanied by the oxidation of carbyne bond, resulting in the first OCCCO-type pentadentate chelates (Scheme 2).

Results and Discussion

Initially, we tested the reactions of carbolong complex **1** with alkynes in the presence of pyridine *N*-oxide. Optimization of the conditions showed complexes **2** could be obtained when **1** and alkynes were performed with 2 equivalents of pyridine *N*-oxide in dichloromethane (DCM) at room temperature (RT) for 2 h (Scheme 3). Various alkynes were tested, but only those bearing an electron-donating group performed well. The yields of complexes **2-1**, **2-2** and **2-3** were 75%, 52% and 71%, respectively, after the purification by column chromatography on silica gel. The results further confirmed that the alkynes with stronger electron-donating groups performed better. All the products were characterized by multinuclear NMR spectroscopy and elemental analysis (Supporting Information). The signals of the substituent group R in alkynes are found at δ 0.91—1.51 in the ^{1}H NMR spectrum and at δ 13.87, 22.82, 30.10, 33.75 in the ^{13}C NMR spectrum for complex **2-1** (^{n}Bu); δ 3.23, 3.26 in the ^{1}H NMR spectrum and δ 59.38, 72.21 in the ^{13}C NMR spectrum for complex **2-2** (CH_2OMe), and δ 0.69—1.72 in the ^{1}H NMR spectrum and δ 25.73, 26.47, 32.13, 42.30 in the ^{13}C NMR spectrum for complex **2-3** (Cy). The signals at δ 9.08 (**2-1**), 9.03 (**2-2**), 9.20 (**2-3**) in the ^{1}H NMR spectra and δ 203.70 (**2-1**), 202.40 (**2-2**), 204.12 (**2-3**) in the ^{13}C NMR spectra can be assigned to the aldehyde groups (C^{10}*H* and C^{10}). The signals of C^{8} and C^{9} groups locate at the range of typical double bonds. For example, for complex **2-1**, the C^{8}*H* is observed at δ 6.70 in its ^{1}H NMR spectrum, and the C^{8} and C^{9} signals display at δ 150.53 and 133.72 in its ^{13}C NMR spectrum. The characteristic features of metal carbyne signals were observed at δ 329.62, 329.42 and 329.99 in the ^{13}C NMR spectra for complexes **2-1**, **2-2** and **2-3**, respectively, at a very down-shifted field. The carbyne signals along with other signals in the metallacycle are similar as those in our previously reported metallapentalynes.[6d,8]

Scheme 3 Reactions of carbolong complex **1** with terminal alkynes in the presence of pyridine *N*-oxide

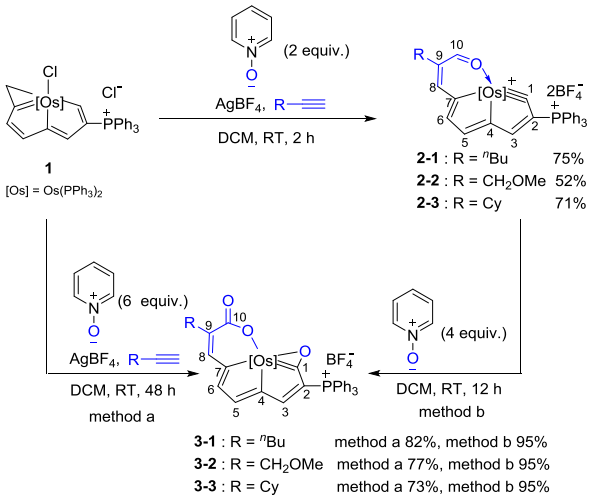

The structure of complex **2-1** was further confirmed by single-crystal X-ray diffraction. As shown in Figure 1, C1—C10 along with Os1 and O1 make up the tricyclic framework. The nearly coplanar tricyclic rings are indicated by the small mean deviation from the least-squares plane (0.072 Å). The bond lengths of C8—C9 (1.368 Å), C9—C10 (1.459 Å) and C10—O1 (1.237 Å) suggest its typical α,β-unsaturated aldehyde structure. The aldehyde oxygen is coordinated to Os1 (Os1—O1: 2.111 Å), forming a six-member

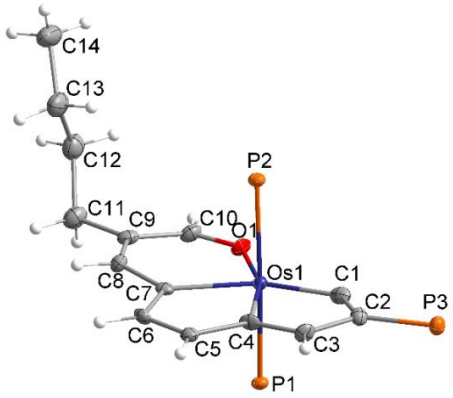

Figure 1 X-ray molecular structure of complex **2-1**. Thermal ellipsoids are set at 50% probability level. The counter ions and phenyl groups in PPh_3 moieties are omitted for clarity.

metallacycle. The C—C bond lengths of the fused five-membered rings (C1—C2 1.382, C2—C3 1.413, C3—C4 1.392, C4—C5 1.384, C5—C6 1.402 and C6—C7 1.410 Å) are almost equal and intermediate between those of typical C=C and C—C bonds, indicating its aromatic structure. All these data along with Os1—C1 distance (1.857 Å) and Os1—C1—C2 angle (129.8°), are comparable to those in the known aromatic osmapentalyne complexes.[6d,8]

DFT calculations were used to illustrate the mechanism for the generation of **2-1**. Initially, we tried a path akin to path a shown in Scheme 1. However, a β-H elimination transition state (TS) could not be located, which might be attributed to the rigid four-membered metallacycle fragment of the intermediate (see S18 for details). We then turned our attention to the new pathway. As shown in Scheme 4, the chlorine in complex **1** is grabbed by Ag^{+} firstly, and meanwhile the alkyne binds to the osmium to form intermediate **1A**. Next, an insertion of the triple bond to the C—Os bond occurs *via* the transition state $\mathbf{TS_{1A\text{-}1B}}$ to form intermediate **1B** by overcoming a barrier of 12.2 kcal·mol^{-1}. Such insertion has also been reported before.[7] Then a pyridine *N*-oxide is coordinated to osmium to form intermediate **1C** in order to meet the 18-electron rule. At the same time, another pyridine *N*-oxide binds to the molecular through hydrogen bond to form intermediate **1D**. Subsequently, the only sp^{3} carbon in the metallacycle is oxidized by the pyridine *N*-oxide to generate **1E**, pyridine and H_2O through $\mathbf{TS_{1D\text{-}1E}}$ with an activation energy of 10.2 kcal·mol^{-1}. The carbene bond next to the phosphonium group is prone to be converted into carbyne bond in such a system by releasing a proton when the osmium bears a positive charge referring to our previous reports.[6d,9] In this case, the elimination of the protonated pyridine *N*-oxide through $\mathbf{TS_{1E\text{-}1F}}$ with an activation energy of 14.6 kcal·mol^{-1} leads to the formation of osmapentalyne **1F**. We speculate that trace amount acid in the solution might catalyze the two C—H bond activation steps. Finally, the metal carbene bond is oxidized by another molecule of pyridine *N*-oxide to form the product **2-1** *via* transition states $\mathbf{TS_{1F\text{-}1G}}$ and $\mathbf{TS_{1G\text{-}2\text{-}1}}$ with activation energy of 8.4 kcal·mol^{-1} and 6.6 kcal·mol^{-1}, respectively. The results reveal the detailed oxygen atom transfer processes during the reactions.

It is noteworthy that overoxidation is a constant problem in terminal alkyne oxidation reactions since the aldehyde products are very reductive. While surprisingly, stepwise oxidations can be achieved in our systems by controlling the amount of pyridine *N*-oxide, even if there are extremely active groups toward oxidants, including aldehyde and the strained cyclic metal carbyne bond, in complexes **2**. As shown in Scheme 3, a series of complexes **3** were prepared by the reactions of complexes **2** with 4 equivalents of pyridine *N*-oxide. Alternatively, complexes **3** could be afforded directly from **1**, $AgBF_4$, alkynes and 6 equivalents of

Scheme 4 Gibbs free-energy profiles for the possible mechanism to the formation of complex **2-1** from **1** calculated by DFT methods

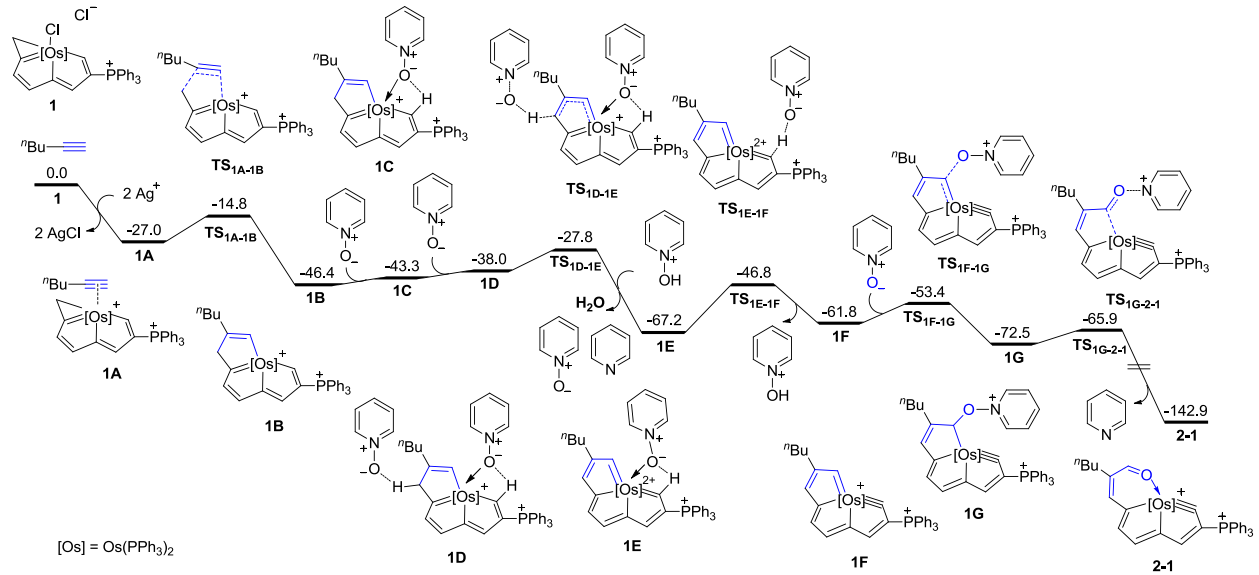

pyridine *N*-oxide. Complexes **3** were characterized by multinuclear NMR spectroscopy and elemental analysis (Supporting Information). The carboxyl (C^{10}) signals are observed at δ 168.10 (**3-1**), 166.25 (**3-2**) and 167.77 (**3-3**) in the ^{13}C NMR spectra. Other signals in the metallapentalene rings are comparable to those in our previously reported metallapentalenes, thus details are not going to be discussed here.[10]

The solid-state structure of complex **3-2** is shown in Figure 2. C1—C10 along with O1, O3 and Os1 make up the tetracyclic framework. Similar to **2-1**, the tetracyclic ring is almost coplanar as well, supported by the small mean deviation from the least-squares plane (0.115 Å). The bond lengths of C10—O1 (1.292 Å) and C10—O2 (1.229 Å) suggest its carboxyl property. The osmapentalene cycle is also aromatic, indicated by the delocalized C—C bond lengths (C1—C2 1.415, C2—C3 1.396, C3—C4 1.416, C4—C5 1.392, C5—C6 1.384 and C6—C7 1.384 Å). All these bond lengths along with Os1—C1 (1.973 Å) are in the range of those in previously reported aromatic osmapentalene complexes.[10] There is a metallaoxirene moiety in complex **3-2**, in which the bond distances of Os1—O3 and C1—O3 are 2.403 Å and 1.238 Å, respectively, suggesting it can also be presented as the resonance structure **3B** (Scheme 5). Anyway, we hold the view that **3A** contributes more according to the NMR data of C^1 (δ 225.16, 224.35 and 225.25 for **3-1**, **3-2** and **3-3**, respectively), together with the requirement for their aromaticity. We previously suggested that the planar tetradentate and pentadentate chelates might also be included in the family of pincer complexes,[6a,11] therefore, **3** can be regarded as the first OCCCO-type pincer complexes.

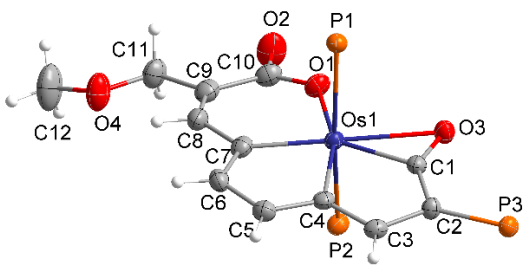

Figure 2 X-ray molecular structure of complex **3-2**. Thermal ellipsoids are set at 50% probability level. The counter ions and phenyl groups in PPh_3 moieties are omitted for clarity.

Scheme 5 Two major resonance structures of **3**.

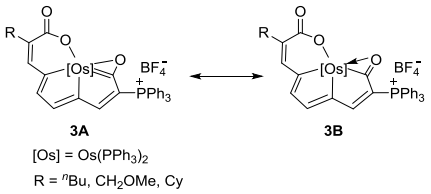

After the success on isolation of a series of novel complexes from the reactions of **1** and pyridine *N*-oxide with terminal alkynes, we further tested its reactivity with an internal alkyne, and a different pathway was discovered. As shown in Scheme 6, the triple bond of dimethyl but-2-ynedioate was broken, oxidized into carboxyl, and coordinated to the osmium. Note that C≡C bond cleavage couldn't occur without the osmium carbolong complex, which indicated that the osmium played an important role. We speculated it might enhance the oxidation ability of the *N*-oxide, but the precise mechanism is required for further investigation. Generally, oxidative cleavage of alkynes to carboxylic acids needs strong oxidants, such as OsO_4 or HIO_4. To our knowledge, there was only one example reported before using pyridine *N*-oxide as the oxidant, in which the carboxylic acids were by-products.[12] Complex **4** was fully characterized by multinuclear NMR spectroscopy, elemental analysis and single-crystal X-ray diffraction (Supporting Information and Figure 3).

Scheme 6 Reaction of carbolong complex **1** with dimethyl but-2-ynedioate in the presence of pyridine *N*-oxide

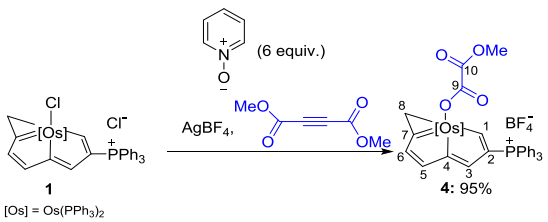

Conclusions

In summary, several oxygen atom transfer reactions between terminal alkynes, osmium carbolong **1** and pyridine *N*-oxide were

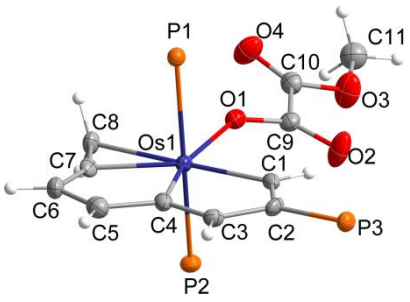

Figure 3 X-ray molecular structure of complex **4**. Thermal ellipsoids are set at 50% probability level. The counter ions and phenyl groups in PPh_3 moieties are omitted for clarity.

investigated. Stepwise oxidations of alkynes were achieved, which yielded aldehyde- and carboxylic acid-coordinated osmium complexes **2** and **3**, respectively. Such processes were discovered in organometallic systems for the first time, and complexes **3** are unprecedented OCCCO-type pentadentate chelates. Furthermore, DFT calculations were performed to illustrate the mechanism for the generation of complex **2-1**, disclosing a new route in oxygen atom transfer reactions between heteroarene *N*-oxides and terminal alkynes. These results might provide an inspiration for new catalytic reactions involving such oxygen atom transfer processes.

Experimental

All syntheses were carried out under an inert atmosphere (N_2) using standard Schlenk techniques, unless otherwise stated. Solvents were distilled under N_2 from sodium/benzophenone (diethyl ether) or calcium hydride (dichloromethane). Complex **1** was synthesized according to published literatures.[13] Other reagents were used as received from commercial sources without further purification. Column chromatography was performed on alumina gel (200—300 mesh) or silica gel (200—300 mesh) in air. Nuclear magnetic resonance (NMR) spectroscopic experiments were performed on a Bruker AVIII-600 spectrometer at room temperature. ^{1}H NMR and ^{13}C NMR chemical shifts are relative to tetramethylsilane, and ^{31}P NMR chemical shifts are relative to 85% H_3PO_4. The absolute values of the coupling constants are given in Hertz (Hz). Multiplicities are abbreviated as singlet (s), doublet (d), triplet (t), multiplet (m) and broad (br). Elemental analyses were performed on a Vario EL III elemental analyzer.

Synthesis and characterization of complex 2-1. A mixture of **1** (300 mg, 0.261 mmol), $AgBF_4$ (152 mg, 0.783 mmol), pyridine-*N*-oxide (49.6 mg, 0.522 mmol) and 1-hexyne (64.3 mg, 0.783 mmol) was stirred at RT in dichloromethane (10 mL) for 2 h to yield a blue suspension. The solid precipitate was removed by filtration, and the solvent was reduced to approximately 5 mL under vacuum and purified by column chromatography on silica gel (eluent: dichloromethane/acetone = 4 : 1) to afford complex **2-1** as a blue solid. Yield: 227 mg, 75%. ^{1}H NMR (600.1 MHz, CD_2Cl_2) δ: 9.56 (d, ^3J(HH) = 3.66 Hz, 1H, C^5*H*), 9.08 (s, 1H, C^{10}*H*), 8.87 (d, ^3J(HP) = 1.02 Hz, 1H, C^3*H*), 8.41 (dt, ^3J(HH) = 3.66 Hz, ^4J(HP) = 3.66 Hz, 1H, C^6*H*), 7.01—7.87 (45H, Ph), 6.70 (s, 1H, C^8*H*), 0.91—1.51 (9H, ^{n}Bu). ^{31}P NMR (242.9 MHz, CD_2Cl_2) δ: 8.83 (t, ^4J(PP) = 5.68 Hz, C*P*Ph$_3$), –1.20 (d, ^4J(PP) = 5.68 Hz, Os*P*Ph$_3$). ^{13}C NMR (150.9 MHz, CD_2Cl_2, plus ^{13}C DEPT-135, ^{1}H-^{13}C HSQC and ^{1}H-^{13}C HMBC) δ: 329.62 (dt, ^2J(CP) = 14.22 Hz, ^2J(CP) = 14.22 Hz, C^1), 215.98 (t, ^2J(CP) = 9.33 Hz, C^7), 203.70 (s, C^{10}), 180.21 (d, ^3J(CP) = 23.33 Hz, C^4), 162.95 (t, ^3J(CP) = 5.40 Hz, C^6), 161.62 (d, ^2J(CP) = 14.53 Hz, C^3), 159.31 (s, C^5), 150.53 (s, C^8), 118.12—136.04 (Ph), 133.72 (s, C^9), 133.38 (dt, ^1J(CP) = 92.30 Hz, ^3J(CP) = 5.47 Hz, C^2), 33.75, 30.10, 22.82, 13.87 (s, ^{n}Bu). Anal. Calcd (%) for $C_{68}H_{59}B_2F_8OOsP_3$: C, 70.49; H, 5.13. Found: C, 69.88; H, 5.142.

Synthesis and characterization of complex 2-2. A mixture of **1** (300 mg, 0.261 mmol), $AgBF_4$ (152 mg, 0.783 mmol), pyridine-*N*-oxide (49.6 mg, 0.522 mmol) and dimethyl 3-methoxyprop-1-yne (54.9 mg, 0.783 mmol) was stirred at RT in dichloromethane (10 mL) for 2 h to yield a blue suspension. The solid precipitate was removed by filtration, and the solvent was reduced to approximately 5 mL under vacuum and purified by column chromatography on silica gel (eluent: dichloromethane/acetone = 4 : 1) to afford complex **2-2** as a blue solid. Yield: 156 mg, 52%. ^{1}H NMR (600.1 MHz, CD_2Cl_2) δ: 9.60 (d, ^3J(HH) = 3.65 Hz, 1H, C^5*H*), 9.03 (s, 1H, C^{10}*H*), 8.97 (d, ^3J(HP) = 0.99 Hz, 1H, C^3*H*), 8.39 (dt, ^3J(HH) = 3.65 Hz, ^4J(HP) = 3.65 Hz, 1H, C^6*H*), 6.96—7.83 (45H, Ph), 6.73 (s, 1H, C^8*H*), 3.26 (s, 3H, C*H*$_3$), 3.23 (s, 2H, OC*H*$_2$). ^{31}P NMR (242.9 MHz, CD_2Cl_2) δ: 8.75 (t, ^4J(PP) = 5.83 Hz,C*P*Ph$_3$), –0.92 (d, ^4J(PP) = 5.83 Hz, Os*P*Ph$_3$). ^{13}C NMR (150.9 MHz, CD_2Cl_2, plus ^{13}C DEPT-135, ^{1}H-^{13}C HSQC and ^{1}H-^{13}C HMBC) δ: 329.42 (dt, ^2J(CP) = 14.74 Hz, ^2J(CP) = 14.74 Hz, C^1), 214.23 (t, ^2J(CP) = 9.23 Hz, C^7), 202.40 (s, C^{10}), 181.40 (d, ^3J(CP) = 23.66 Hz, C^4), 163.48 (t, ^3J(CP) = 5.55 Hz, C^6), 162.46 (d, ^2J(CP) = 14.62 Hz, C^3), 158.58 (s, C^5), 150.81 (s, C^8), 118.04—136.07 (Ph), 134.30 (d, ^1J(CP) = 84.50 Hz, C^2), 129.57 (s, C^9), 72.21 (s, OCH_2), 59.38 (s, CH_3). Anal. Calcd (%) for $C_{66}H_{55}B_2F_8O_2OsP_3$: C, 69.13; H, 4.83. Found: C, 69.00; H, 4.897.

Synthesis and characterization of complex 2-3. A mixture of **1** (300 mg, 0.261 mmol), $AgBF_4$ (152 mg, 0.783 mmol), pyridine-*N*-oxide (49.6 mg, 0.522 mmol) and ethynylcyclohexane (84.7 mg, 0.783 mmol) was stirred at RT in dichloromethane (10 mL) for 2 h to yield a blue suspension. The solid precipitate was removed by filtration, and the solvent was reduced to approximately 5 mL under vacuum and purified by column chromatography on silica gel (eluent: dichloromethane/acetone = 4 : 1) to afford complex **2-3** as a blue solid. Yield: 220 mg, 71%. ^{1}H NMR (600.1 MHz, CD_2Cl_2) δ: 9.37 (d, ^3J(HH) = 3.84 Hz, 1H, C^5*H*), 9.20 (s, 1H, C^{10}*H*), 8.81 (d, ^3J(HP) = 0.72 Hz, 1H, C^3*H*), 8.34 (dt, ^3J(HH) = 3.84 Hz, ^4J(HP) = 3.84 Hz, 1H, C^6*H*), 6.98—7.84 (45H, Ph), 6.78 (s, 1H, C^8*H*), 0.69—1.72 (11H, Cy). ^{31}P NMR (242.9 MHz, CD_2Cl_2) δ: 8.71 (t, ^4J(PP) = 5.83 Hz,C*P*Ph$_3$), –1.13 (d, ^4J(PP) = 5.83 Hz, Os*P*Ph$_3$). ^{13}C NMR (150.9 MHz, CD_2Cl_2, plus ^{13}C DEPT-135, ^{1}H-^{13}C HSQC and ^{1}H-^{13}C HMBC) δ: 329.99 (dt, ^2J(CP) = 15.14 Hz, ^2J(CP) = 15.14 Hz, C^1), 215.72 (t, ^2J(CP) = 9.41 Hz, C^7), 204.12 (s, C^{10}), 179.97 (d, ^3J(CP) = 21.71 Hz, C^4), 163.06 (t, ^3J(CP) = 5.50 Hz, C^6), 161.18 (d, ^2J(CP) = 16.10 Hz, C^3), 158.75 (s, C^5), 150.03 (s, C^8), 138.53 (s, C^9), 118.15—136.05 (Ph), 133.24 (dt, ^1J(CP) = 92.70 Hz, ^2J(CP) = 5.25 Hz, C^2), 42.30, 32.13, 26.47, 25.73 (s, Cy). Anal. Calcd (%) for $C_{70}H_{61}B_2F_8OOsP_3$: C, 70.96; H, 5.19. Found: C, 70.65; H, 5.38.

Synthesis and characterization of complex 3-1. **Method a**: A mixture of **1** (300 mg, 0.261 mmol), $AgBF_4$ (152 mg, 0.783 mmol), pyridine-*N*-oxide (149 mg, 1.57 mmol) and dimethyl 1-hexyne (64.3 mg, 0.783 mmol) was stirred at RT in dichloromethane (10 mL) for 48 h to yield a blue suspension. The solid precipitate was removed by filtration, and the solvent was reduced to approximately 5 mL under vacuum and purified by column chromatography on neutral alumina (eluent: dichloromethane/acetone = 4 : 1) to afford complex **3-1** as a blue solid. Yield: 277 mg, 82%. **Method b**: A mixture of **2-1** (300 mg, 0.222 mmol) and pyridine-*N*-oxide (127 mg, 1.33 mmol) was stirred at RT in dichloromethane (10 mL) for 12 h to yield a blue solution. The solvent was reduced to approximately 3 mL under vacuum, then diethyl ether (20 mL) was added to the solution. The blue precipitate was collected by filtration and washed with Et_2O (2×15 mL) to give **3-1** as a blue solid. Yield: 273 mg, 95%. ^{1}H NMR (600.1 MHz, CD_2Cl_2) δ: 8.36 (s, 1H, C^5*H*), 8.22 (s, 1H, C^3*H*), 7.28 (s, 1H, C^6*H*), 7.12—7.74 (45H, Ph), 5.82 (s, 1H, C^8*H*), 0.75—1.41 (9H, ^{n}Bu). ^{31}P NMR (242.9 MHz, CD_2Cl_2) δ: 9.02 (s, C*P*Ph$_3$), 1.10 (s, Os*P*Ph$_3$). ^{13}C NMR (150.9 MHz, CD_2Cl_2, plus ^{13}C DEPT-135, ^{1}H-^{13}C HSQC and ^{1}H-^{13}C HMBC) δ: 226.42 (t, ^2J(CP) = 6.26 Hz, C^7), 225.16 (dt, ^2J(CP) = 4.45 Hz, ^2J(CP) = 4.45 Hz, C^1), 186.31 (d, ^3J(CP) = 23.71 Hz, C^4), 168.10 (s, C^{10}), 163.98 (d, ^2J(CP) = 16.06 Hz, C^3), 162.86 (s, C^5), 150.21 (s, C^6), 141.13 (s, C^9), 139.55 (s, C^8), 119.23—135.43 (Ph), 101.53 (d, ^1J(CP) = 88.85 Hz, C^2), 33.45, 30.17, 23.18, 14.18 (s, ^{n}Bu). Anal. Calcd (%)

for $C_{68}H_{58}BF_4O_3OsP_3$: C, 63.16; H, 4.52. Found: C, 62.78; H, 5.152.

Synthesis and characterization of complex 3-2. **Method a**: A mixture of **1** (300 mg, 0.261 mmol), $AgBF_4$ (152 mg, 0.783 mmol), pyridine-*N*-oxide (149 mg, 1.57 mmol) and 3-methoxyprop-1-yne (54.9 mg, 0.783 mmol) was stirred at RT in dichloromethane (10 mL) for 48 h to yield a blue suspension. The solid precipitate was removed by filtration, and the solvent was reduced to approximately 5 mL under vacuum and purified by column chromatography on neutral alumina (eluent: dichloromethane/acetone = 4 : 1) to afford complex **3-2** as a blue solid. Yield: 257 mg, 77%. **Method b**: A mixture of **2-2** (300 mg, 0.224 mmol) and pyridine-*N*-oxide (128 mg, 1.57 mmol) was stirred at RT in dichloromethane (10 mL) for 12 h to yield a blue solution. The solvent was reduced to approximately 3 mL under vacuum, then diethyl ether (20 mL) was added to the solution. The blue precipitate was collected by filtration and washed with Et_2O (2×15 mL) to give **3-2** as a blue solid. Yield: 273 mg, 95%. ^{1}H NMR (600.1 MHz, CD_2Cl_2) δ: 8.31 (d, ^3J(HH) = 3.38 Hz, 1H, C^5*H*), 8.21 (d, ^3J(HP) = 2.79 Hz, 1H, C^3*H*), 7.36 (s, 1H, C^6*H*), 7.09—7.74 (45H, Ph), 6.05 (s, 1H, C^8*H*), 3.14 (s, 3H, C*H*$_3$), 3.11 (s, 2H, OC*H*$_2$). ^{31}P NMR (242.9 MHz, CD_2Cl_2) δ: 9.09 (s, C*P*Ph$_3$), 1.24 (s, Os*P*Ph$_3$). ^{13}C NMR (150.9 MHz, CD_2Cl_2, plus ^{13}C DEPT-135, ^{1}H-^{13}C HSQC and ^{1}H-^{13}C HMBC) δ: 225.06 (t, ^2J(CP) = 6.73 Hz, C^7), 224.35 (dt, ^2J(CP) = 4.50 Hz, ^2J(CP) = 4.50 Hz, C^1), 186.46 (dt, ^3J(CP) = 23.94 Hz, ^2J(CP) = 3.50 Hz, C^4), 166.25 (s, C^{10}), 164.31 (d, ^2J(CP) = 15.36 Hz, C^3), 162.49 (s, C^5), 150.37 (s, C^6), 137.86 (s, C^8), 136.30 (s, C^9), 118.76—135.10 (Ph), 101.58 (d, ^1J(CP) = 88.96 Hz, C^2), 71.55 (s, OC*H*$_2$), 58.57 (s, C*H*$_3$). Anal. Calcd (%) for $C_{66}H_{54}BF_4O_4OsP_3$: C, 61.88; H, 4.26. Found: C, 61.63; H, 4.537.

Synthesis and characterization of complex 3-3. **Method a**: A mixture of **1** (300 mg, 0.261 mmol), $AgBF_4$ (152 mg, 0.783 mmol), pyridine-*N*-oxide (149 mg, 1.57 mmol) and ethynylcyclohexane (84.7 mg, 0.783 mmol) was stirred at RT in dichloromethane (10 mL) for 48 h to yield a blue suspension. The solid precipitate was removed by filtration, and the solvent was reduced to approximately 5 mL under vacuum and purified by column chromatography on neutral alumina (eluent: dichloromethane/ acetone = 4 : 1) to afford complex **3-3** as a blue solid. Yield: 251 mg, 73%. **Method b**: A mixture of **2-3** (300 mg, 0.218 mmol) and pyridine-*N*-oxide (124 mg, 1.308 mmol) was stirred at RT in dichloromethane (10 mL) for 12 h to yield a blue solution. The solvent was reduced to approximately 3 mL under vacuum, then diethyl ether (20 mL) was added to the solution. The blue precipitate was collected by filtration and washed with Et_2O (2×15 mL) to give **3-3** as a blue solid. Yield: 273 mg, 95%. ^{1}H NMR (600.1 MHz, CD_2Cl_2) δ: 8.30 (d, ^3J(HH) = 3.82 Hz, 1H, C^5*H*), 8.29 (d, ^3J(HH) = 3.09 Hz, 1H, C^3*H*), 7.23 (s, 1H, C^6*H*), 7.07—7.75 (45H, Ph), 6.00 (s, 1H, C^8*H*), 0.45—1.56 (11H, Cy). ^{31}P NMR (242.9 MHz, CD_2Cl_2) δ: 8.99 (s, C*P*Ph$_3$), 0.56 (s, Os*P*Ph$_3$). ^{13}C NMR (150.9 MHz, CD_2Cl_2, plus ^{13}C DEPT-135, ^{1}H-^{13}C HSQC and ^{1}H-^{13}C HMBC) δ: 227.08 (m, C^7), 225.25 (m, C^1), 185.85 (m, C^4), 167.77 (s, C^{10}), 163.13 (d, ^2J(CP) = 16.01 Hz, C^3), 162.93 (s, C^5), 150.89 (s, C^6), 146.25 (s, C^9), 138.97 (s, C^8), 119.30—135.41 (Ph), 101.49 (d, ^1J(CP) = 90.46 Hz, C^2), 41.27, 32.81, 27.07, 26.81 (s, Cy). Anal. Calcd (%) for $C_{70}H_{60}BF_4O_3OsP_3$: C, 63.73; H, 4.58. Found: C, 63.96; H, 5.571.

Synthesis and characterization of complex 4. A mixture of **1** (300 mg, 0.261 mmol), $AgBF_4$ (152 mg, 0.783 mmol), pyridine-*N*-oxide (149 mg, 1.57 mmol) and dimethyl but-2-ynedioate (74.2 mg, 0.522 mmol) was stirred at RT in dichloromethane (10 mL) for 24 h to yield a yellow suspension. The solid precipitate was removed by filtration, and the filtrate was washed with Na_2CO_3 aqueous solution and the organic phase was evaporated under vacuum to approximately 3 mL, then diethyl ether (20 mL) was added to the solution. The yellow precipitate was collected by filtration and washed with Et_2O (2×15 mL) to give **4** as a yellow solid. Yield: 315 mg, 95%. ^{1}H NMR (600.1 MHz, CD_2Cl_2) δ: 15.52 (d, ^3J(HP) = 17.08 Hz, 1H, C^1*H*), 9.06 (d, ^3J(HH) = 3.00 Hz, 1H, C^5*H*), 8.58 (t, ^4J(HP) = 2.63 Hz, 1H, C^3*H*), 6.98—7.84 (45H, Ph), 6.65 (m, 1H, C^6*H*), 3.63 (s, 3H, OC*H*$_3$), 3.06 (s, 2H, C^8*H*). ^{31}P NMR (242.9 MHz, CD_2Cl_2) δ: 11.55 (s, C*P*Ph$_3$), –3.32 (s, Os*P*Ph$_3$). ^{13}C NMR (150.9 MHz, CD_2Cl_2, plus ^{13}C DEPT-135, ^{1}H-^{13}C HSQC and ^{1}H-^{13}C HMBC) δ: 242.84 (m, C^7), 241.66 (m, C^1), 191.65 (d, ^3J(CP) = 24.14 Hz, C^4), 166.54 (s, C^5), 165.06 (s, C^9), 161.99 (s, C^{10}), 150.59 (d, ^2J(CP) = 25.65 Hz, C^3), 144.92 (s, C^6), 119.95—135.08 (Ph), 135.72 (d, ^1J(CP) = 70.53 Hz, C^2), 52.34 (s, OC*H*$_3$), 26.84 (s, C^8). Anal. Calcd (%) for $C_{65}H_{54}BF_4O_4OsP_3$: C, 61.52; H, 4.29. Found: C, 61.03; H, 3.947.

Crystallographic analysis. All single crystals suitable for X-ray diffraction were grown from dichloromethane solution layered with hexane. Single-crystal X-ray diffraction data were collected on a Rigaku XtaLAB Synergy, Dualflex, HyPix diffractometer with mirror-monochromated Cu Kα radiation (λ = 1.54184 Å) for **2-1** and Mo Kα radiation (λ = 0.71073 Å) for **3-2** and **4**. The crystal was kept at 100.00 K during data collection. With Olex2,[14] the structure was solved using the ShelXT[15] structure solution program and refined with the ShelXL[16] refinement package using least-squares minimisation. Non-H atoms were refined anisotropically unless otherwise stated. Hydrogen atoms were introduced at their geometric positions and refined as riding atoms unless otherwise stated. CCDC-1977108 (**2-1**), CCDC-1977117 (**3-2**), CCDC-1977118 (**4**), contain the supplementary crystallographic data for this paper. Some bad reflections of (Iobs-Icalc)/SigmaW > 10 were omitted in **2-1**. The alert level B in the checkCIF report of **2-1** was caused by the heavy atom effect of osmiun atom. Absorbtion correction was done, but it didn't works. Beam stop mask of dual source diffractometer blocked some reflections in **3-2**, resulting in the alert level B in the checkCIF report, but it doesn't affect the structure analysis. These data can be obtained free of charge from the Cambridge Crystallographic Data Centre *via* www.ccdc.cam.ac.uk /data_request/cif.

Computational details. All of the structures evaluated were optimized at the M06-2X/6-31G* level of DFT[17] with an SDD basis set[18] to describe P, Cl, Ag and Os atoms; thermal corrections were calculated at the same level. Vibrational frequencies were also calculated at the same level to confirm that all minima have no imaginary frequency and each transition state has only one. Single-point energies were calculated at the M06-2X/def2-TZVP level,[19] in conjunction with the SMD solvation model using dichloroethane as the solvent.[20] Intrinsic reaction coordinate (IRC) calculations were performed to ensure that each transition state connected two particular minima. All the above calculations were performed using the Gaussian 09 software package.[21]

Supporting Information

The supporting information for this article is available on the WWW under https://doi.org/10.1002/cjoc.202000227.

Acknowledgement

We gratefully acknowledge the Guangdong Provincial Key Laboratory of Catalysis (No. 2020B121201002) and NSFC (Nos. U1705254 and 21931002) for their financial support.

References

[1] For reviews, see: (a) Petrosyan, A.; Hauptmann, R.; Pospech, J. Heteroarene *N*-oxides as Oxygen Source in Organic Reactions. *Eur. J. Org. Chem*. **2018**, 5237–5252; (b) Zheng, Z.; Wang, Z.; Wang, Y.; Zhang, L. Au-Catalysed oxidative cyclisation. *Chem. Soc. Rev*. **2016**, *45*, 4448–4458; (c) Yeom, H.-S.; Shin, S. Catalytic Access to alpha-Oxo Gold Carbenes by N-O Bond Oxidants. *Acc. Chem. Res*. **2014**, *47*, 966–977; (d) Zhang, L. A Non-Diazo Approach to α-Oxo Gold Carbenes *via* Gold-Catalyzed Alkyne Oxidation. *Acc. Chem. Res*. **2014**, *47*, 877–888; (e) Xiao, J.; Li, X. Gold α-Oxo Carbenoids in Catalysis: Catalytic Oxy-

gen-Atom Transfer to Alkynes. *Angew*. *Chem*. *Int*. *Ed*. **2011**, *50*, 7226–7236.

[2] For select articles: (a) Zhao, Q.; Henrion, G.; Gagosz, F. Synthesis of isochroman-4-ones and 2*H*-pyran-3(6*H*)-ones by gold-catalyzed oxidative cycloalkoxylation of alkynes. *Bioorg*. *Med*. *Chem*. **2019**, *27*, 2616–2620; (b) Wagh, S. B.; Singh, R. R.; Sahani, R. L.; Liu, R.-S. Gold-Catalyzed Oxidative Hydrative Alkenylations of Propargyl Aryl Thioethers with Quinoline *N*-oxides Involving a 1,3-Sulfur Migration. *Org*. *Lett*. **2019**, *21*, 2755–2758; (c) Wagh, S. B.; Sharma, P.; Patil, M. D.; Liu, R.-S. Gold-catalyzed oxidative cycloalkenations of alkynes with quinoline *N*-oxides. *Org*. *Chem*. *Front*. **2019**, *6*, 226–230; (d) Xu, Z.; Zhai, R.; Liang, T.; Zhang, L. Efficient One-Pot Multifunctionalization of Alkynes en Route to α-Alkoxyketones, α-Thioketones, and α-Thio Thioketals by Using an Umpolung Strategy. *Chem*. *Eur*. *J*. **2017**, *23*, 14133–14137; (e) Huang, W.; Xiang, J.; He, W. Gold-catalyzed Synthesis of 4-(2-Oxoalkoxy) butyl Methanesulfonates *via* Ring-opening of Tetrahydrofuran. *Chem*. *Lett*. **2014**, *43*, 893–894; (f) Xu, M.; Ren, T.-T.; Wang, K.-B.; Li, C.-Y. Synthesis of Cyclobutanones via Gold-Catalyzed Oxidative Rearrangement of Homopropargylic Ethers. *Adv*. *Synth*. *Catal*. **2013**, *355*, 2488–2494; (g) Shi, S.; Wang, T.; Yang, W.; Rudolph, M.; Hashmi, A. S. K. Gold-Catalyzed Synthesis of Glyoxals by Oxidation of Terminal Alkynes: One-Pot Synthesis of Quinoxalines. *Chem*. *Eur*. *J*. **2013**, *19*, 6576–6580; (h) Xu, M.; Ren, T.-T.; Li, C.-Y. Gold-Catalyzed Oxidative Rearrangement of Homopropargylic Ether via Oxonium Ylide. *Org*. *Lett*. **2012**, *14*, 4902–4905; (i) He, W.; Xie, L.; Xu, Y.; Xiang, J.; Zhang, L. Electrophilicity of α-oxo gold carbene intermediates: halogen abstractions from halogenated solvents leading to the formation of chloro/bromomethyl ketones. *Org*. *Biomol*. *Chem*. **2012**, *10*, 3168–3171; (j) Ye, L.; He, W.; Zhang, L. A Flexible and Stereoselective Synthesis of Azetidin-3-ones through Gold-Catalyzed Intermolecular Oxidation of Alkynes. *Angew*. *Chem*. *Int*. *Ed*. **2011**, *50*, 3236–3239; (k) Ye, L.; He, W.; Zhang, L. Gold-Catalyzed One-Step Practical Synthesis of Oxetan-3-ones from Readily Available Propargylic Alcohols. *J*. *Am*. *Chem*. *Soc*. **2010**, *132*, 8550–8551; (l) Ye, L.; Cui, L.; Zhang, G.; Zhang, L. Alkynes as Equivalents of α-Diazo Ketones in Generating α-Oxo Metal Carbenes: A Gold-Catalyzed Expedient Synthesis of Dihydrofuran-3-ones. *J*. *Am*. *Chem*. *Soc*. **2010**, *132*, 3258–3259.

[3] (a) Alvarez-Perez, A.; Esteruelas, M. A.; Izquierdo, S.; Varela, J. A.; Saa, C. Ruthenium-Catalyzed Oxidative Amidation of Alkynes to Amides. *Org*. *Lett*. **2019**, *21*, 5346–5350; (b) Zhang, W.-W.; Gao, T.-T.; Xu, L.-J.; Li, B.-J. Macrolactonization of Alkynyl Alcohol through Rh(I)/Yb(III) Catalysis. *Org*. *Lett*. **2018**, *20*, 6534–6538; (c) Rong, M.-G.; Qin, T.-Z.; Liu, X.-R.; Wang, H.-F.; Zi, W. De Novo Synthesis of Phenols and Naphthols through Oxidative Cycloaromatization of Dienynes. *Org*. *Lett*. **2018**, *20*, 6289–6293; (d) Zeng, H.; Li, C.-J. A Complete Switch of the Directional Selectivity in the Annulation of 2-Hydroxybenzaldehydes with Alkynes. *Angew*. *Chem*. *Int*. *Ed*. **2014**, *53*, 13862–13865; (e) Wang, Y.; Zheng, Z.; Zhang, L. Ruthenium-Catalyzed Oxidative Transformations of Terminal Alkynes to Ketenes by Using Tethered Sulfoxides: Access to β-Lactams and Cyclobutanones. *Angew*. *Chem*. *Int*. *Ed*. **2014**, *53*, 9572–9576; (f) Kim, I.; Roh, S. W.; Lee, D. G.; Lee, C. Rhodium-Catalyzed Oxygenative [2 + 2] Cycloaddition of Terminal Alkynes and Imines for the Synthesis of β-Lactams. *Org*. *Lett*. **2014**, *16*, 2482–2485; (g) Kim, I.; Lee, C. Rhodium-catalyzed oxygenative addition to terminal alkynes for the synthesis of esters, amides, and carboxylic acids. *Angew*. *Chem*. *Int*. *Ed*. **2013**, *52*, 10023–10026; (h) Pati, K.; Liu, R.-S. Efficient syntheses of α-pyridones and 3(2*H*)-isoquinolones through ruthenium-catalyzed cycloisomerization of 3-en-5-ynyl and o-alkynylphenyl nitrones. *Chem*. *Commun*. **2009**, 5233–5235.

[4] Gronnier, C.; Kramer, S.; Odabachian, Y.; Gagosz, F. Cu(I)-Catalyzed Oxidative Cyclization of Alkynyl Oxiranes and Oxetanes. *J*. *Am*. *Chem*. *Soc*. **2012**, *134*, 828–831.

[5] Hung, H.-H.; Liao, Y.-C.; Liu, R.-S. Oxidant-Dependent Chemoselectivity in the Gold-Catalyzed Oxidative Cyclizations of 3,4,6,6-Tetrasubstituted 3,5-Dien-1-ynes. *J*. *Org*. *Chem*. **2013**, *78*, 7970–7976.

[6] (a) Zhu, C.; Xia, H. Carbolong Chemistry: A Story of Carbon Chain Ligands and Transition Metals. *Acc*. *Chem*. *Res*. **2018**, *51*, 1691–1700; (b) Hua, Y.; Zhang, H.; Xia, H. Aromaticity: History and Development. *Chin*. *J*. *Org*. *Chem*. **2018**, *38*, 11–28; (c) Wang, H.; Zhou, X.; Xia, H. Metallaaromatics Containing Main-Group Heteroatoms. *Chin*. *J*. *Chem*. **2018**, *36*, 93–105; (d) Zhu, C.; Li, S.; Luo, M.; Zhou, X.; Niu, Y.; Lin, M.; Zhu, J.; Cao, Z.; Lu, X.; Wen, T.; Xie, Z.; Schleyer, P. v. R.; Xia, H. Stabilization of anti-aromatic and strained five-membered rings with a transition metal. *Nat*. *Chem*. **2013**, *5*, 698–703.

[7] (a) Zhu, C.; Yang, C.; Wang, Y.; Lin, G.; Yang, Y.; Wang, X.; Zhu, J.; Chen, X.; Lu, X.; Liu, G.; Xia, H. CCCCC pentadentate chelates with planar Möbius aromaticity and unique properties. *Sci*. *Adv*. **2016**, *2*, e1601031; (b) Zhu, C.; Wu, J.; Li, S.; Yang, Y.; Zhu, J.; Lu, X.; Xia, H. Synthesis and characterization of a metallacyclic framework with three fused five-membered rings. *Angew*. *Chem*. *Int*. *Ed*. **2017**, *56*, 9067–9071.

[8] Li, J.; Kang, H.; Zhuo, K.; Zhuo, Q.; Zhang, H.; Lin, Y.-M.; Xia, H. Alternation of Metal-Bridged Metallacycle Skeletons: From Ruthenapentalyne to Ruthenapentalene and Ruthenaindene Derivative. *Chin*. *J*. *Chem*. **2018**, *36*, 1156–1160.

[9] Zhu, C.; Yang, Y.; Wu, J.; Luo, M.; Fan, J.; Zhu, J.; Xia, H. Five-Membered Cyclic Metal Carbyne: Synthesis of Osmapentalynes by the Reactions of Osmapentalene with Allene, Alkyne, and Alkene. *Angew*. *Chem*. *Int*. *Ed*. **2015**, *54*, 7189–7192.

[10] (a) Lin, J.; Ding, L.; Zhuo, Q.; Zhang, H.; Xia, H. Formal [2 + 2 + 2] Cycloaddition Reaction of a Metal–Carbyne Complex with Nitriles: Synthesis of a Metallapyrazine Complex. *Organometallics* **2019**, *38*, 2264–2271; (b) Zhu, Q.; Zhu, C.; Deng, Z.; He, G.; Chen, J.; Zhu, J.; Xia, H. Synthesis and Characterization of Osmium Polycyclic Aromatic Complexes *via* Nucleophilic Reactions of Osmapentalyne. *Chin*. *J*. *Chem*. **2017**, *35*, 628–634.

[11] Zhuo, Q.; Zhang, H.; Ding, L.; Lin, J.; Zhou, X.; Hua, Y.; Zhu, J.; Xia, H. Rhodapentalenes: Pincer Complexes with Internal Aromaticity. *iScience* **2019**, *19*, 1214–1224.

[12] Xu, J.-h.; Wu, W.-b.; Wu, J. Photoinduced Divergent Alkylation/Acylation of Pyridine *N*-oxides with Alkynes under Anaerobic and Aerobic Conditions. *Org*. *Lett*. **2019**, *21*, 5321–5325.

[13] Zhu, C.; Zhou, X.; Xing, H.; An, K.; Zhu, J.; Xia, H. σ-Aromaticity in an Unsaturated Ring: Osmapentalene Derivatives Containing a Metallacyclopropene Unit. *Angew*. *Chem*. *Int*. *Ed*. **2015**, *54*, 3102–3106.

[14] Dolomanov, O. V.; Bourhis, L. J.; Gildea, R. J.; Howard, J. A. K.; Puschmann, H. OLEX2: a complete structure solution, refinement and analysis program. *J*. *Appl*. *Cryst*. **2009**, *42*, 339–341.

[15] Sheldrick, G. M. SHELXT-Integrated Space-Group and Crystal-Structure Determination. *Acta Cryst*. **2015**, *A71*, 3–8.

[16] Sheldrick, G. M. Crystal Structure Refinement with SHELXL. *Acta Cryst*. **2015**, *C71*, 3–8.

[17] (a) Zhao, Y.; Truhlar, D. G. The M06 suite of density functionals for main group thermochemistry, thermochemical kinetics, noncovalent interactions, excited states, and transition elements: two new functionals and systematic testing of four M06-class functionals and 12 other functionals. *Theor*. *Chem*. *Acc*. **2008**, *120*, 215–241; (b) Hariharan, P. C.; Pople, J. A. The influence of polarization functions on molecular orbital hydrogenation energies. *Theor*. *Chim*. *Acta* **1973**, *28*, 213–222.

[18] (a) Andrae, D.; Häußermann, U.; Dolg, M.; Stoll, H.; Preuß, H. Energy-adjustedab initio pseudopotentials for the second and third row transition elements. *Theor*. *Chim*. *Acta* **1990**, *77*, 123–141; (b) Dolg, M.; Wedig, U.; Stoll, H.; Preuss, H. Energy-adjusted *ab initio* pseudopotentials for the first row transition elements. *J*. *Chem*. *Phys*. **1987**, *86*, 866–872.

[19] Weigend, F.; Ahlrichs, R. Balanced basis sets of split valence, triple zeta valence and quadruple zeta valence quality for H to Rn: Design and assessment of accuracy. *Phys*. *Chem*. *Chem*. *Phys*. **2005**, *7*, 3297–3305.

[20] Marenich, A. V.; Cramer, C. J.; Truhlar, D. G. Universal Solvation Model Based on Solute Electron Density and on a Continuum Model

of the Solvent Defined by the Bulk Dielectric Constant and Atomic Surface Tensions. *J. Phys. Chem. B* **2009**, *113*, 6378–6396.

[21] Frisch, M. J.; Trucks, G. W.; Schlegel, H. B.; Scuseria, G. E.; Robb, M. A.; Cheeseman, J. R.; Scalmani, G.; Barone, V.; Mennucci, B.; Petersson, G. A.; Nakatsuji, H.; Caricato, M.; Li, X.; Hratchian, H. P.; Izmaylov, A. F.; Bloino, J.; Zheng, G.; Sonnenberg, J. L.; Hada, M.; Ehara, M.; Toyota, K.; Fukuda, R.; Hasegawa, J.; Ishida, M.; Nakajima, T.; Honda, Y.; Kitao, O.; Nakai, H.; Vreven, T.; Montgomery, J. A.; Peralta, Jr., J. E.; Ogliaro, F.; Bearpark, M.; Heyd, J. J.; Brothers, E.; Kudin, K. N. V. N.; Staroverov, Keith, T.; Kobayashi, R.; Normand, J.; Raghavachari, K.; Rendell, A.; Burant, J. C.; Iyengar, S. S.; Tomasi, J.; Cossi, Rega, N.; Millam, J. M.; Klene, M.; Knox, J. E.; Cross, J. B.; Bakken, V.; Adamo, C.; Jaramillo, J.; Gomperts, R.; Stratmann, R. E.; Yazyev, O.; Austin, A. J.; Cammi, R.; Pomelli, C.; Ochterski, J. W.; Martin, R. L.; Morokuma, K.; Zakrzewski, V. G.; Voth, G. A.; Salvador, P.; Dannenberg, J. J.; Dapprich, S.; Daniels, A. D.; Farkas, O.; Foresman, J. B.; Ortiz, J. V.; Cioslowski, J.; Fox, D. J. *Gaussian 09*, revision B.01, Gaussian, Inc., Wallingford CT, **2009**.

Manuscript received: April 21, 2020
Manuscript revised: June 1, 2020
Manuscript accepted: June 2, 2020
Accepted manuscript online: June 8, 2020
Version of record online: XXXX, 2020

